PHYSICAL REVIEW B VOLUME 27, NUMBER 6 15 MARCH 1983

Self-consistent pseudopotential calculation of the electronic structure of PdH and Pd_4H

C. T. Chan and Steven G. Louie
Department of Physics, University of California, Berkeley, California 94720
(Received 29 November 1982)

The electronic structure of PdH and Pd_4H is studied in detail with a fully self-consistent pseudopotential approach using a mixed basis set. The band structure, density of states, angular-momentum-decomposed density of states, and charge densities are analyzed for both systems. Particular attention has been paid to the nature of the Pd—H bonding state and the effect of changing the hydrogen concentration as we go from PdH to Pd_4H. Agreements with experimental data and previous calculations on PdH are very good. The essential physical nature of the hydride system is summarized in a simple conceptual picture which should be applicable to substoichiometric PdH_x and other hydrides for the prediction of Fermi-surface properties.

I. INTRODUCTION

The metal-hydrogen system has received a great deal of interest and attention in the last decade. There is a rich literature on the subject.[1–4] In particular, the palladium-hydrogen system has been studied heavily both experimentally and theoretically. However, detailed understanding of the electronic properties is achieved only after realistic band-structure calculations are applied. This approach was pioneered by Switendick.[5] The effort has been carried on by other authors, using different approaches. Today we have knowledge about both stoichiometric and nonstoichiometric PdH, their electronic structure, heat of formation, superconductivity, and other properties.[1–4]

Chemisorption of H on Pd surfaces has also been studied in detail, and there has been in some cases good agreement between theoretical and experimental results. However, there are still mysteries which stand unanswered. A good example is the recently observed temperature dependency of the angle-resolved photoemission data on hydrogen chemisorption on transition-metal surfaces.[6] As has been reported in the literature, hydrogen chemisorbed on the Pd(111) surface produces a split-off peak in the photoemission spectra due to Pd—H bonding very similar to that of the bulk β-phase PdH observed by Eastman *et al.*[7] However, the hydrogen-induced peak disappears from the spectrum when the experiment is performed at room temperature, although measurements indicate that there is still at least half a monolayer of hydrogen present.[6] Eberhardt *et al.*[6] attempted to explain this paradoxical situation by proposing that the hydrogen atoms may migrate into subsurface octahedral sites when the temperature is raised to room temperature. In this model the subsurface sites are proposed to have lower energy. The surface sites are occupied instead in low temperature because of an energy barrier. Since the experimental photoemission spectra show hydrogen-induced peaks below the Pd d bands whether the hydrogen is chemisorbed on the surface or forming a β-phase hydride at the bulk, the interpretation of Eberhardt *et al.* is valid only if the bonding of H with Pd at subsurface sites has very different characters when compared with that at bulk and surface sites.

Elucidation of such subtle properties needs a very careful study and comparison of the electronic structure of the three separate cases: bulk, subsurface, and surface. The surface chemisorption calculation has been done successfully using a fully self-consistent mixed-basis pseudopotential approach.[8] The present work uses the same formalism to treat the hydride (PdH and Pd_4H) problem. Very good agreement with both experimental and previous calculations is obtained for PdH, which has been extensively studied. For Pd_4H only electronic eigenvalues have been reported by Switendick,[9] but bonding characters of the Pd—H bond and Fermi-surface properties are actually of more physical interest. These are discussed in the present paper. The comparison of the substoichiometric Pd_4H with PdH furnishes us with information about the change induced in the hydride system as H concentration changes. This may also provide us with insight into the studies of subsurface chemisorption, as Pd with hydrogen absorbed at subsurface sites can be regarded as a dilute hydride.

The rigid-band model has been used successfully in the study of Pd hydrides but it is now known that the underlying assumption [that the density of states (DOS) of Pd is not changed during hydride formation] is incorrect. We include in this paper a discussion of a simple model which treats the Pd-H interaction more accurately and can give predictions of the Fermi-surface properties of various hydride systems.

The paper is organized in the following way: In Sec. II the calculation procedures are described. In Sec. III we present the main results which include the band structure, density of states (DOS), localized density of states (LDOS) at each atomic site and their angular momentum decompositions, charge densities, and bonding characteristics for both systems. In Sec. IV a simple conceptual picture of transition-metal hydrides is discussed. Section V is the summary and conclusion.

II. CALCULATION

The stoichiometric palladium hydride has rock-salt (NaCl) structure such that the palladium atoms form a fcc lattice with the hydrogen atoms filling up all the octahedral sites. There are two atoms in the primitive unit cell. Experimentally, the lattice is known to be isotropically expanded in this β phase.[10] In this calculation the lattice constant is expanded by 6% with respect to the pure Pd value of 3.89 Å. For Pd_4H we have assumed an ordered structure, the unit cell is cubic with Pd atoms at (0,0,0), $(\frac{1}{2},\frac{1}{2},0)$, $(\frac{1}{2},0,\frac{1}{2})$, and $(0,\frac{1}{2},\frac{1}{2})$ (in units of the primitive translation vectors), and one hydrogen atom at $(\frac{1}{2},\frac{1}{2},\frac{1}{2})$, the center of the unit cell. The lattice constant is expanded by 2% from that of the pure Pd value.

The band structures of both systems were calculated by the mixed-basis pseudopotential method.[11] The pseudopotential Hamiltonian we used is

$$H=\frac{1}{2m}P^2+V_{\rm ps}+V_H+V_{\rm xc}\ , \tag{1}$$

where

$$V_{\rm ps}=\sum_{\vec{R},\vec{\tau}_a} V_a^{\rm ion}(\vec{r}-\vec{R}_i-\vec{\tau}_a)$$

is a superposition of ionic pseudopotentials. $\vec{R}_i$ refers to lattice vectors; $\vec{\tau}_a$ refers to the basis vectors in the unit cell.

The palladium ionic pseudopotential is a nonlocal (nonrelativistic) pseudopotential of the form

$$V_{\rm Pd}^{\rm ion}=\sum_{l=0}^{2} V_l\hat{P}_l\ , \tag{2}$$

where $\hat{P}_l$ is the lth angular momentum projection operator and V_l has the analytical form in real space (in atomic units)

$$V_l=\frac{-10}{r}\tanh(\sqrt{\alpha_0}r)+C_l e^{-\alpha_l r^2}\ . \tag{3}$$

The potential parameters are tabulated in Table I.

The hydrogen ionic pseudopotential is a local potential fitted to the analytical form in Fourier space

$$V(q)=\frac{a_1}{q^2}(\cos a_2 q+a_3)e^{a_4 q^4}\ . \tag{4}$$

The potential parameters are also listed in Table I. These potentials have been used previously to give very good results in bulk and surface calculations.[8,11,12]

Both the Hartree potential (V_H) and the exchange correlation potential ($V_{\rm xc}$) are functionals of the charge density $\rho(\vec{r})$ which is given by

$$\rho(\vec{r})=2\sum_{n,\vec{k}} |\psi_{n,\vec{k}}|^2\Theta(\epsilon_F-\epsilon_{n,\vec{k}})\ , \tag{5}$$

where n is the band index, $\vec{k}$ are k points in the Brillouin zone (BZ), ϵ_F is the Fermi energy, $\epsilon_{n,\vec{k}}$ are the eigenvalues, and Θ is the step function.

The Hartree potential V_H is determined by the pseudo-charge-density through the Poisson equation

$$\nabla^2 V_H(\vec{r})=-4\pi e^2\rho(\vec{r})\ . \tag{6}$$

The Hedin-Lundquist local exchange correlation[13] was used for $V_{\rm xc}$, i.e.,

$$V_{\rm xc}=-\frac{e^2}{\pi}(3\pi^2\rho)^{1/3}\beta\ , \tag{7}$$

where β is the correlation enhancement and has the functional form of

TABLE I. Potential parameters for Pd and H (in atomic units).

	α_0	C_1	C_2	C_3	α_1	α_2	α_3
Pd	1.0	3.125	3.125	−10.85	0.8	0.8	1.1

	a_1	a_2	a_3	a_4
H	23.3273	0.2800	−1.5380	−0.0070

$$\beta(r_s)=1+0.7734x \ln\left[1+\frac{1}{x}\right]$$

with $x=r_s/21$. [$r_s=(3/4\pi n)^{1/3}$, where n is the electron density.]

The self-consistent procedure has been discussed in detail elsewhere.[14] The special points scheme of Chadi and Cohen[15] was employed. At each iteration ten k points in the irreducible Brillouin zone (IBZ) were computed for PdH while four k points were computed for Pd_4H. Self-consistency is said to be obtained when the input and output potential differs by less than 2 mRy.

The main feature of the mixed-basis approach is to expand the wave function in plane waves as well as Gaussian orbitals localized at atomic sites. In this particular problem the electron wave function of the system is expanded in the form

$$\psi_{n\vec{k}}(\vec{r})=\frac{1}{\sqrt{\Omega}}\sum_{\vec{G}} a_n(\vec{k}+\vec{G})\exp[i(\vec{k}+\vec{G})\cdot\vec{r}] + \sum_{\mu} b_{n\mu}(\vec{k})\phi_\mu(\vec{k},\vec{r}) , \quad (8)$$

where $\vec{G}$ is a reciprocal lattice vector, n is the band index, and Ω is the crystal volume. The local orbital basis functions are given by

$$\phi_\mu=\frac{1}{\sqrt{\Omega}}\sum_{\vec{R}_i}\exp[i\vec{k}\cdot(\vec{R}_i+\vec{\tau}_{Pd})] \times d_\mu(\vec{r}-\vec{R}_i-\vec{\tau}_{Pd}) , \quad (9)$$

where $\vec{R}_i$ is a lattice vector, $\vec{\tau}_{Pd}$ is a basis vector at the Pd sites, and the d_μ's are functions of the form $r^2e^{-\lambda r^2}Y_{2m}(\theta,\phi)$.

Thus the ϕ's are a Bloch sum of localized orbitals centered around the Pd sites. These orbitals are used to model the localized behavior of the Pd d electrons. Such a mixed-basis set is very suitable for transition metals and their compounds which have highly extended electrons as well as localized d states. Their versatility has been demonstrated in previous calculations.[8,11]

In the present calculation plane waves up to $|\vec{k}+\vec{G}|^2$ equal to 7.0 Ry are included in the plane-wave set. The localized functions ϕ's are also expanded in plane waves of reciprocal-lattice vectors when the matrix elements are computed (see Ref. 11 for details) and plane waves up to $|\vec{k}+\vec{G}|^2$ equal to 30 Ry were included in the expansion of the ϕ's.

III. RESULTS

A. Band structure and density of states

The band structure of PdH along some high-symmetry directions is plotted in Fig. 1. Figure 2(a) shows the total DOS of PdH. The DOS was determined by the linear tetrahedron method of Lehmann and Taut.[16] 256 tetrahedra in the IBZ have been used in the interpolation procedure which corresponds to 89 k points in the IBZ. All the eigenvalues at these k points were determined from first principles. For comparison purposes we have plotted in Fig. 2(b) the DOS of pure Pd that we have calculated.

The DOS of Pd_4H is shown in Fig. 2(c). The eigenvalues for 20 k points on a regular mesh in the IBZ are calculated from first principles. We fit to the calculated data (using linear-least-square fit) a function containing symmetrized Fourier functions of the form

$$\epsilon_n(\vec{k})=\sum_m b_m(n)\left[\sum_\alpha \exp[i\vec{k}\cdot(\alpha\vec{R}_m)]\right] , \quad (10)$$

where $\vec{R}_m$ is a real-space lattice vector and α is an element of the point group $\mathcal{G}$. The set $\{\alpha\vec{R}_m: \alpha\in\mathcal{G}\}$ forms a star in the real space and n is the band index. The DOS is then determined by the linear tetrahedron method with 216 tetrahedra in the IBZ, corresponding to 84 k points in the IBZ. The

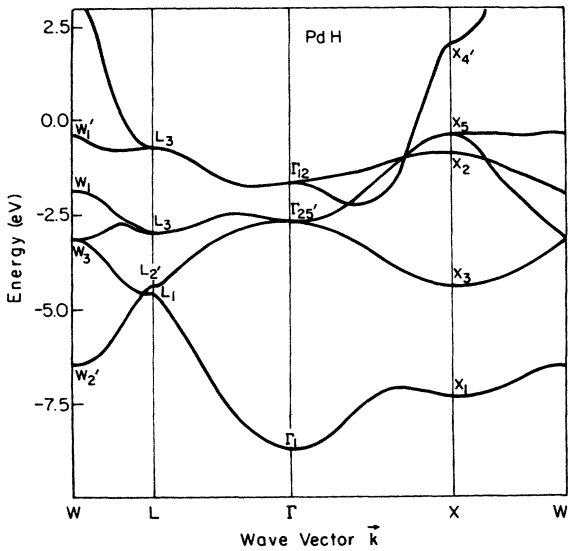

FIG. 1. Energy bands for PdH along some high-symmetry directions (Fermi level at 0 eV).

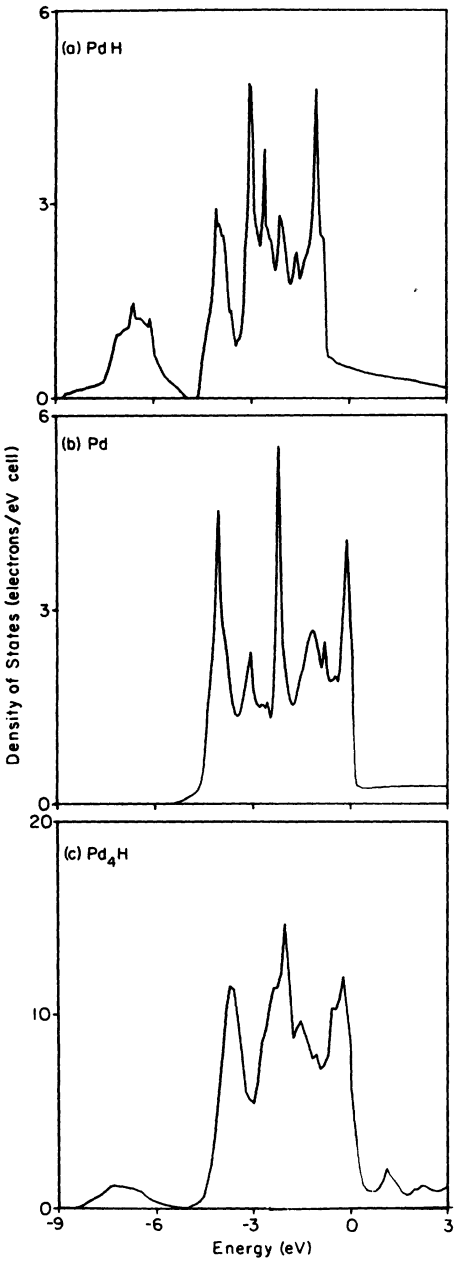

FIG. 2. Density of states for (a) PdH, (b) Pd, and (c) Pd_4H. The Fermi level is at 0 eV.

eigenvalues of these points are generated with Eq. (10).

The band structure of PdH (Fig. 1) agrees very well with previous calculations.[9,17–21] In Table II we compare the energy differences of some energy eigenvalues at high-symmetry k points with those of Switendick,[9] Zbasnik and Mahnig,[17] Papaconstantopoulos *et al.*,[18,19] and Gupta and Freeman.[20] [All the above previous results are from augmented-plane-wave (APW) calculations.] There are minor discrepancies among different calculations, which reflects the different approaches and approximations used by different authors such as self-consistency, inclusion of relativistic effects, and choice of exchange and correlation potential. The choice of lattice constants also affects the resuts. We note from Table II that the characteristic bandwidths of Zbasnik and Mahnig's results are larger than those of Papaconstantopoulos *et al.*, which in turn are larger than ours, whereas the lattice constant chosen goes in the opposite direction. As a test we have repeated the calculation with a somewhat smaller lattice expansion of 2% for PdH and the energy differences do expand almost uniformly (see Table II). The DOS's we have obtained are very similar to those of Gupta and Freeman[20] and to those of Papaconstantopoulos *et al.*[18]

From an examination of the band structure and DOS of PdH, we immediately notice the following major changes due to hydride formation:

(1) The "d-band manifold" of PdH has a narrower width than that of Pd and contains fewer electron states. Thus states are depleted from the d-band region when Pd interacts with hydrogen.

(2) A band is formed below the bottom of the palladium d bands. This band corresponds to the bonding state between Pd and H.

(3) The Fermi energy is shifted upward relative to the Pd d band. The d-band holes are filled and states of s-p character above the d-band edge are occupied. This upward shift greatly reduces the DOS at the Fermi energy (E_F).

Quantitative agreements are obtained when we compare the DOS with photoemission experiments. The ultraviolet photoemission measurement of Eastman *et al.*[7] shows a strong emission from d-band states within $\sim$4.4 eV of E_F. The d-band width from the calculated DOS is about 4.2 eV. Thus agreement is good. The most important feature in the photoemission experiment is the observation of a conspicuous hydrogen-induced level. Eastman *et al.* found a peak around 3—4 eV wide centered at about 5.4 eV below E_F, while Antonangeli *et al.*[22] found a peak at about 6 eV below E_f. The bonding Pd-H band from our calculation is 3.88 eV wide in good agreement with experiments. It is positioned at around 6.5 eV below E_F, which is lower in energy than the experimental result of Eastman *et al.* It is interesting to note that most of the previous calculations of stoichiometric PdH also have the hydride-induced peak about 1 eV or more lower than the result of Eastman *et al.* Various authors have attributed this to concentration effects, as the experimental sample is probably $PdH_{0.6}$, not PdH. The APW virtual-crystal approximation calculations of

TABLE II. Comparison of energy differences (in Ry) of eigenvalues at high-symmetry k points. The first row shows the percentage increase of the lattice constant of PdH with respect to Pd. Data of Switendick, Zbasnik-Mahnig, and Papaconstantopoulos *et al.* is adapted from Table I of Ref. 18.

Lattice expansion	Switendick[a] ~3.6%	Zbasnik-Mahnig[b] ~3.6%	Papaconstantopoulos *et al.*[c] ~5%	Gupta-Freeman[d] ~5%	Present[e] 6%	Present[f] 2%
Γ_{12}-Γ'_{25}	0.085	0.103	0.092	~0.08	0.075	0.101
Γ'_{25}-Γ_1	0.423	0.631	0.546	~0.5	0.445	0.482
Γ_1-Γ_1	1.558	1.462	1.554		1.50	1.681
X_1-X_1	0.910	~0.98	0.936		0.882	0.989
L_1-L_1	0.824	~0.85	0.754		0.660	0.748
X_5-X_1	0.504	0.731	~0.57	~0.56	0.509	0.551
X_5-X_3	0.307	0.353	0.333	~0.3	0.294	0.314

[a]APW (Ref. 9).
[b]APW (Ref. 17)
[c]APW (Ref. 18).
[d]APW (Ref. 20). Values estimated from their published band structure.
[e]Present self-consistent pseudopotential calculation with 6% lattice expansion.
[f]Present self-consistent pseudopotential calculation with 2% lattice expansion.

Zbasnik and Mahnig indicate that the bonding state comes closer to the Fermi energy as concentration is decreased. Our calculation shows the contrary. The DOS of Pd_4H of our calculation shows that the position of the bonding state is at approximately the same position with respect to the Fermi energy [see Fig. 2(c)], even though the concentration is substantially decreased. This is consistent with the more recent results of coherent-potential approximation (CPA) calculations.[19]

An examination of the DOS of Pd_4H shows that it is rather similar to that of PdH. The dispersion of the lowest band is slightly decreased to ~3.5 eV while the d-band region is increased to ~4.6 eV. The d-band region of Pd_4H resembles that of pure Pd, with the characteristic three-peak structure. There are two distinct differences between PdH and Pd_4H. We note first that the DOS for the bonding states has diminished magnitude relative to the d states. This is a direct consequence of lower hydrogen concentration as one hydrogen atom can only interact to form one bonding state. Another important change is the position of the Fermi energy. It is now situated at the d-band edge indicating that there are d-band holes. The antibonding states (the small peak at ~1–2 eV above the Fermi level) are also closer to the d-band edge than those of the PdH.

B. Charge density

Many discussions have been devoted to the protonic, anionic, and covalent-bond models of metal hydrides. The protonic model assumes that the hydrogen atom enters the system as a proton, giving up its electron to the Pd host to fill up the d-band holes. The anionic model assumes that the hydride ion H^- is formed, while the covalent-bond model assumes that the metal and hydrogen form covalent bonds. Details of these models can be found elsewhere.[1–4] Both theoretical and experimental studies have now established that these models are oversimplified. The nature of the bond will become more apparent when we examine charge-density plots of PdH and Pd_4H in this section which are lacking in the literature.

The valence charge densities have been defined by Eq. (5). We plot the valence charge densities of pure Pd in Fig. 3(a) and that of PdH in Fig. 3(b). Both of them are for a (100) plane. When these two plots are compared, we notice that a small amount of charge is transferred from the region between the neighboring Pd atoms to the regions between two nearest-neighbor Pd and H atoms. To study the bonding state more closely, we single out the lowest band of PdH and plot the charge density of that

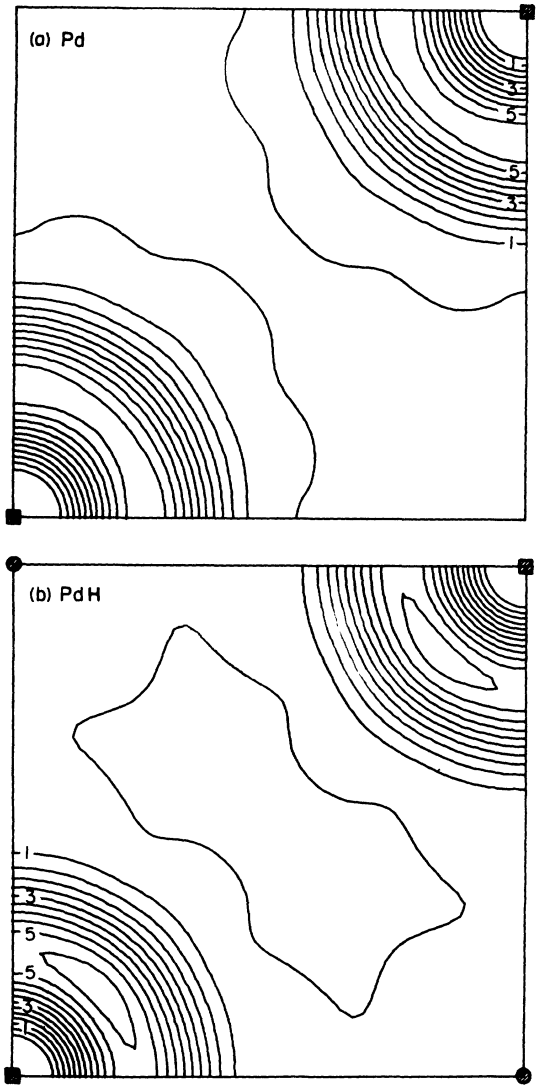

FIG. 3. Charge densities of valence electrons for (a) Pd and (b) PdH in the (100) plane in units of 0.1 electrons/(a.u.)^3. In the figure a square denotes a Pd atom, a circle denotes a H atom.

band in Fig. 4. In Fig. 4 the Pd—H bonding is clearly visible. We can also see that the charge around the Pd site is very much *d*-like, while that around the H site is *s*-like. The charges around both the Pd and H sites are of comparable magnitude, so we cannot speak of protonic or anionic model. To quantify our comments, we have integrated the valence charge density of the lowest (bonding) band around spheres of various radii R about each atom and also about a interstitial site (at the midpoint of two Pd atoms). The results are displayed in Table III. It is interesting to note that the proton is screened by roughly one electron at the radius where

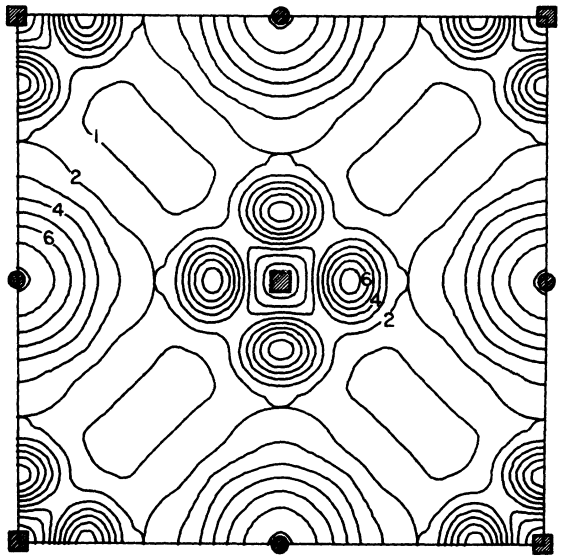

FIG. 4. Charge densities for the lowest (bonding) band of PdH in the (100) plane in units of 0.01 electrons/(a.u.)^3. In the figure a square denotes a Pd atom and a circle denotes a H atom.

the Pd and H spheres touch ($\sim$2 a.u.). The results also show that the hydrogen always has more charge around it than the Pd up to a Wigner-Seitz radius of $\sim$2.4 a.u.

For Pd_4H the charge densities corresponding to the lowest band are plotted in Figs. 5(a) and 5(b), and the integrated charge densities are shown in Table III. Figure 5(a) is a (110) plane containing the diagonal of the cubic cell while Fig. 5(b) is a (100) plane cutting through the center of the cell where the H is situated. The ordered Pd_4H's that we considered have four Pd atoms in the unit cell. Three of them (those on the faces of the cube) are at nearest-neighbor distance from the H atom, while the Pd atom at the cell corner is further away. The charge-density plot in Fig. 5(a) shows that the bonding charge is only shared by the H atom and the Pd atoms at nearest-neighbor sites. The atom at the corner has a negligible share of the bonding charge. This implies that the effective Pd-H interaction is short range and hardly extends beyond nearest neighbor. Despite the change of a Pd to H ratio from 1:1 to 4:1, the charge corresponding to the bonding state around the H atom is very similar for these systems, as can be seen by comparing the charge-density plots and the integrated charge in Table III. This, together with our knowledge of the DOS presented in Sec. III A, leads us to the conclusion that changes in concentration have very little effect on the H atom in PdH_x systems. It is always screened by approximately the same amount of *s*-

TABLE III. Charge (in units of number of electrons) inside a sphere of radius R for the lowest band (bonding band) at three different sites inside the unit cell.

	PdH		
R (a.u.)	Pd (0,0,0)	H $(-\frac{1}{2},\frac{1}{2},\frac{1}{2})$	Interstitial $(\frac{1}{2},0,0)$
1.0	0.11	0.25	0.04
1.2	0.21	0.38	0.07
1.4	0.32	0.53	0.12
1.6	0.41	0.68	0.20
1.8	0.50	0.84	0.32
2.0	0.59	0.99	0.48
2.2	0.71	1.13	0.69
2.4	0.87	1.28	0.96
2.6	1.07	1.45	1.26

	Pd_4H		
R (a.u.)	Pd $(\frac{1}{2},\frac{1}{2},0)$	H $(\frac{1}{2},\frac{1}{2},\frac{1}{2})$	Pd (0,0,0)
1.0	0.03	0.27	~0.0
1.2	0.06	0.42	0.0
1.4	0.09	0.58	0.0
1.6	0.12	0.74	0.01
1.8	0.15	0.91	0.01
2.0	0.19	1.06	0.01
2.2	0.24	1.21	0.01
2.4	0.30	1.35	0.01
2.6	0.38	1.50	0.01

like charges. This can be partly attributed to the fact that the Pd-H interaction is short ranged and the H site has the same number of Pd nearest neighbors as long as we are considering PdH_x where $x<1$. On the other hand, the charge around the Pd atoms for Pd_4H bears less resemblance to that of PdH. The single bonding band of Pd_4H has to be shared by three Pd atoms, and the number of nearest-neighbor H atoms changes. The changes in angular momentum characteristics are difficult to estimate by inspecting the charge densities, but it will be shown in Sec. III C that the charge at the Pd site is still predominately d-like in character for Pd_4H, although the s and p contributions become more important in this case.

C. Local DOS and angular momentum decomposed DOS

From the charge-density plots (Figs. 4 and 5) we can already see that the hydride bonding state involves the d electrons on the Pd sites and the s electrons on the H site. To quantify these remarks we have calculated the local density of states (LDOS) for both the Pd and H sites defined by the following equation:

$$D(\epsilon,\vec{\tau}_i)=2\sum_{n,\vec{k}}\delta(\epsilon-\epsilon_{n,\vec{k}}) \times\int_{\Omega}|\psi_{n,\vec{k}}(\vec{r}-\vec{\tau}_i)|^2dr^3 , \tag{11}$$

where the volume of integration Ω is taken to be a sphere of radius R about the atom at $\vec{\tau}_i$.

We have chosen $R=2.0$ a.u. for Pd and $R=1.5$ a.u. for H. The integrated charges at those radii in the bonding band are approximately the same at the two sites for PdH. The LDOS for the Pd site and the H site in PdH are plotted in Fig. 6. From the plot we immediately see that the hydrogen has the same share of bonding charge as Pd even though we choose a smaller radius for it. The electrons with energy from -5.0 to -0.8 eV are almost entirely centered around the Pd site and they mostly correspond to the palladium d bands. However, a comparison with the d states in pure Pd [Fig. 2(b)] shows variations in shape and peak position so that perturbation by hydrogen is strong. The LDOS is further decomposed into its angular momentum components according to the following equation:

$$D_l(\epsilon,\vec{\tau}_i)=2\sum_{n,\vec{k}}\delta(\epsilon-\epsilon_{n,\vec{k}})C^l_{n,\vec{k}} , \tag{12}$$

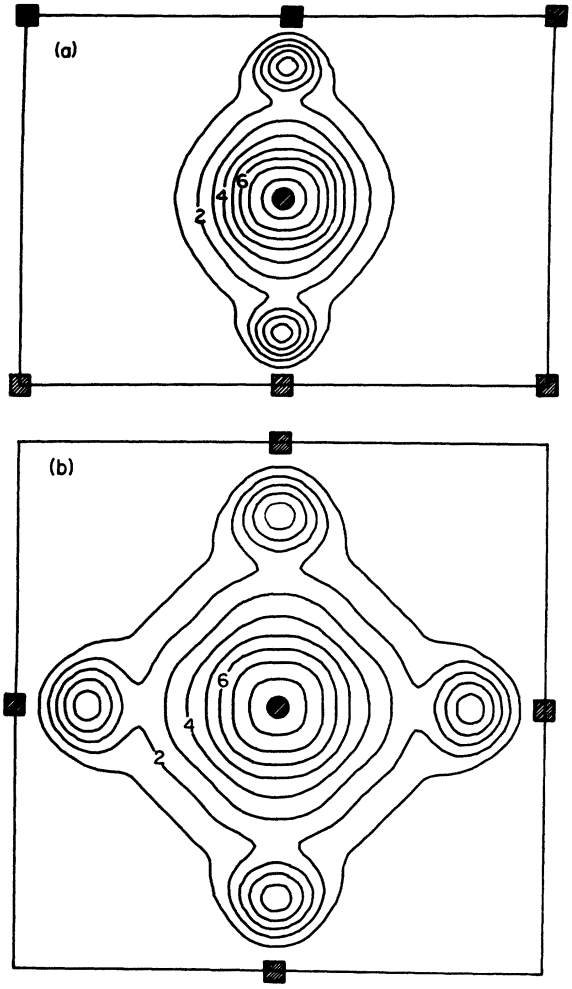

FIG. 5. Charge densities [in 0.01 electrons/(a.u.)^3] for the lowest (bonding) band of Pd_4H in the (a) (110) plane and (b) (100) plane. A square denotes a Pd atom. A circle denotes a H atom. Note that the Pd atoms on the corners of (a) have negligible share of the bonding charge.

where $C^l_{n,\vec{k}}$ is defined as

$$C^l_{n,\vec{k}} = \int_\Omega \psi^*_{n,\vec{k}}(\vec{r}-\vec{\tau}_i)\hat{P}_l\psi_{n,\vec{k}}(\vec{r}-\vec{\tau}_i)dr^3 .$$

$\hat{P}_l$ is the angular momentum projection operator. The D_l's are plotted in Fig. 7 for PdH.

In this problem we need only consider l up to 2. For the hydrogen site we observe that the s component is completely dominant. In particular, the bonding state is almost completely s-like. The p and d contributions are so small they they almost do not show up in the graph. For the range of -5.0 to 0.8 eV, all components of the LDOS of the hydrogen site are virtually negligible. For the Pd site we discovered that the d component is dominant for the

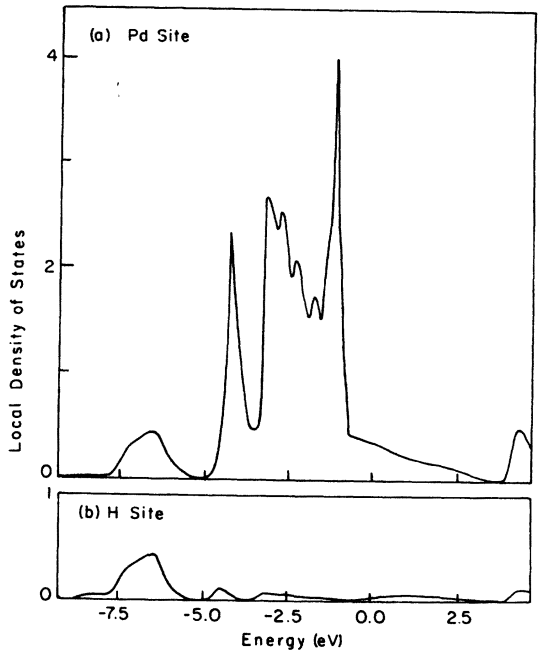

FIG. 6. Local density of states for PdH decomposed at (a) Pd site and (b) H site.

bonding band. The s and p contributions are small, though not negligible. For electron states from -5.0 to -0.8 eV they are predominantly d-like as expected. The qualitative features agree well with the partial DOS analysis of the APW calculation of Gupta and Freeman.[20]

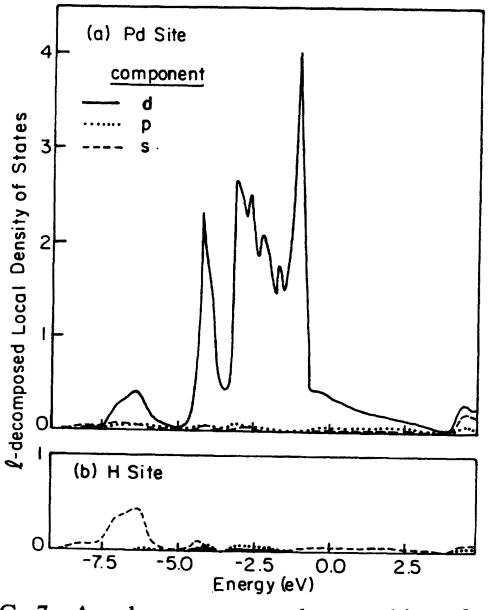

FIG. 7. Angular momentum decomposition of local density of states for PdH at (a) Pd site and (b) H site.

The same angular momentum decomposition procedure was repeated for the bonding band of Pd_4H and the results are depicted in Fig. 8. Figure 8(a) shows the s component of the LDOS of the lowest band at the H site. The s component is again dominant over the p and d components. The p and d contributions are so small that they cannot be plotted in the figure. Figure 8(b) shows the angular momentum characteristics at the Pd site. The d character is still dominant but the s,p contributions are relatively larger compared with those of PdH. However, if we take into account the large change in the Pd to H ratio, the difference in bonding characteristics should be considered small. From these considerations we can confidently assert that the lowest band is an s-d bonding state formed from the interaction of Pd $4d$ and H $1s$ orbitals.

D. DOS at Fermi energy

Both the specific heat and magnetic susceptibility (Pauli) are closely related to the DOS at the Fermi energy. The specific heat and magnetic susceptibility for PdH are known experimentally to be much lower than for pure Pd, which can be attributed to a decrease of DOS at Fermi energy. These quantities

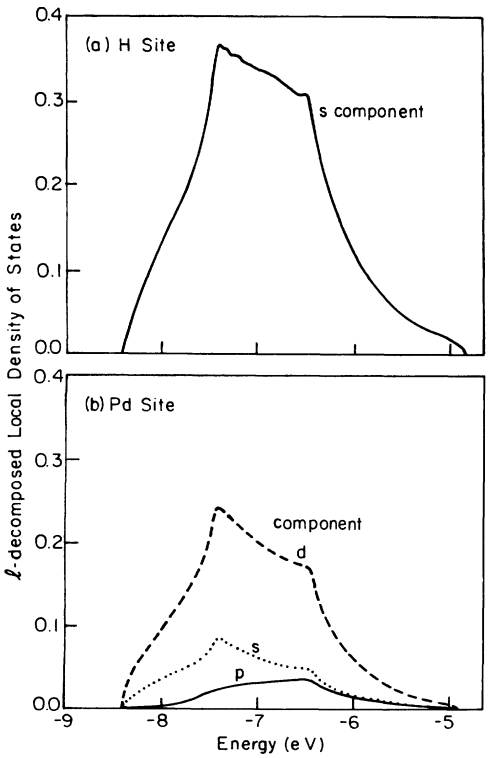

FIG. 8. Angular momentum decomposition of the bonding (lowest) band of Pd_4H at (a) H site and (b) Pd site. For the decomposition at the H site, the p and d components are too small to be plotted on the figure.

can be calculated according to the following formulas[23]:

$$\gamma=\frac{\pi^2}{3}k_B^2 D(E_F)(1+\lambda_\gamma)\,, \tag{13}$$

$$\chi_P=\mu_B^2 D(E_F)(1+\lambda_\chi)\,, \tag{14}$$

where $D(E_F)$ is the DOS at E_F for both spins, λ_γ and λ_χ are enhancement factors due to electron-phonon and electron-electron interactions, k_B is the Boltzmann constant, and μ_B is the Bohr magneton. We obtained a value of $D(E_F)=0.47$ for PdH (in units of electrons/eV cell) in good accordance with Switendick's value of 0.45 and the Papaconstantopoulos *et al.* value of 0.46. Thus the $D(E_F)$ is much lower than that of Pd (which is ~ 2.3), explaining the lowering of the above-mentioned quantities. For Pd_4H the Fermi energy is situated at the d-band edge and the DOS at Fermi energy is found to be 1.85 electrons/eV per Pd atom. This is close to the values of ~ 2.0 (in same units) obtaind by the CPA calculation of Papaconstantopoulos *et al.*[19]

IV. STRONG BONDING MODEL

It has been known for a long time that the rigid-band model has been very successful in explaining experimental results that are closely related to the DOS at E_F, such as the above-mentioned specific heat and magnetic susceptibility. The model assumes that the Pd DOS is not changed during hydride formation. Hydrogen enters the system as a proton, donating its electron to the Pd d bands to fill up the d-band holes. This is consistent with the experimental fact that both the specific heat and the magnetic susceptibility decrease with the increase of hydrogen content, which would lower the DOS at E_F by such a mechanism. Since PdH_x becomes diamagnetic at $x=0.6$, it may be interpreted that there are 0.6 holes in the Pd d band. However, de Haas–van Alphen effect measurements[24] indicate that there are 0.36 holes instead of 0.6 holes. Theoretical calculations since Switendick's work have shown that the protonic model is not correct for transition-metal hydrides. Nevertheless, it can be seen from Fig. 2 that qualitative features of the DOS of Pd and its hydrides are very similar at and close to the d-band edge—all are characterized by a sharp decrease in DOS when the d-band edge is passed. As the E_F is situated at the region where the DOS of the hydride is similar to the host metal, it is not surprising that the rigid-band model gives good qualitative predictions.

As the rigid-band model is essentially an incorrect conceptual model for this system, it is desirable to replace it by a simple conceptual picture that is as simple as the rigid-band model and yet consistent

with our understanding of the problem at this stage. We propose such a model below. We have noted that because of strong interactions between H and the host metal, the effect of hydrogen on the host metal (e.g., Pd) is to deplete states in the d bands and form a split-off bonding state. The antibonding state is far above the Fermi energy as long as the H concentration is high and would not enter into discussion since it is always unoccupied. We first consider the pure metal. The d bands and the s bands should be able to hold a total of $10+\gamma$ electrons up to the d-band edge (ten electrons from the d states and γ electrons from the s states). γ is usually small. For example, Pd has ten electrons but there are 0.36 holes, indicating that $\gamma \sim 0.36$.[24] The situation is illustrated schematically in Fig. 9(a) for Pd. The DOS is based on the Friedel model[25] in which the d states have constant DOS for a range of energy equal to the d-band width. The s states have free-electron-like DOS. When hydrogen is added to form the metal hydride (MH_x), we expect the following changes to be induced in the DOS which is depicted schematically by Fig. 9(b):

(1) Metal-hydrogen bonding states are formed and split off from the d bands. As one hydrogen atom interacts to form one Pd—H bond, the bonding region should contain $2x$ electrons for MH_x.

(2) Electron states are depleted from the d bands by the interaction. Since the number of states depleted should be approximately proportional to x, we can denote the number of depleted states by αx (we expect α to be close to 2). Then, the s-d bands now only hold $10+\gamma-\alpha x$ electrons up to the d-band edge.

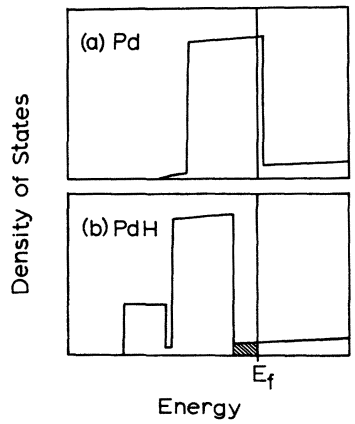

FIG. 9. Schematic DOS for (a) Pd and (b) PdH. (a) Pd: The DOS has contributions from the d states which in the Friedel model is a constant over a range equal to the width of the d bands. They can accommodate a total of ten electrons. The s bands have a free-electron-like DOS and contribute γ electrons up to the d-band edge. (b) PdH_x: The DOS in the strong bonding model has three main regions: (i) A low-lying bonding band with $2x$ electrons; (ii) the "d bands" which can hold $10+\gamma-\alpha x$ electrons; (iii) a total of $\delta(x)$ electron states that are occupied above the d-band edge (shaded region).

(3) The structure of the DOS close to and above the d-band edge is not strongly perturbed by the hydride formation. In that region the DOS of both the metal and its hydride are mainly characterized by a sharp drop from a peak to a relatively flat region of smaller DOS after the d-band edge is passed. For the hydride we denote the number of electron states between the Fermi energy and the d-band edge by $\delta(x)$ [shaded region in Fig. 9(b)]. If $\delta(x)$ is negative, there are holes in the d bands.

For a host metal M with n-valence d electrons, by balancing the number of occupied electron states below the Fermi energy, we arrive at the following equation for a MH_x hydride:

$$2x+(10+\gamma-\alpha x)+\delta(x)=n+x \ . \tag{15}$$

The right-hand side is the total number of valence electrons in the MH_x per unit cell, while the three terms on the left-hand side are the number of electrons in the occupied states in the bonding band, in the s-d bands, and above the d bands, respectively. We will see that Fermi-surface-related properties can be discussed in terms of this simple equation.

fcc transition elements in groups VIII and IB which are adjacent to Pd have very similar band structures and DOS, except for a change in the d-band width and the relative position of the d bands to the s band. Hence the band structure and DOS of their hydrides are expected to be very similar, and thus Eq. (15) should be applicable to them. For stoichiometric hydrides ($x=1$) we may rewrite Eq. (15) as

$$\delta(x=1)=(n-11)+(\alpha-\gamma) \ . \tag{16}$$

The value of $(\alpha-\gamma)$ should not differ drastically for these elements, thus the value of $\delta(x)$ would change mainly through the dependence on the value of n. The change of $\delta(x=1)$ with respect to n is summarized in Table IV, where $(\alpha-\gamma)$ is estimated to be ~ 1.5. The general trend across the Periodic Table can be understood immediately. The negative value of $\delta(x=1)$ for the group Co, Rh, and Ir means that there are still holes in the d band for the hydrides, and the Fermi energy is located in the d bands where the DOS is high. δ is slightly positive for Ni, Pd, and Pt indicating that E_F is at or slightly above the d-band maximum. On the other hand, an increase in the value of δ by 1 as we go to the noble metals (Cu, Ag, and Au) would make the E_F high above the d-band edge as the states of s,p character above the d-band edge have small DOS. These remarks are indeed borne out by other calculations.[26,27] These

TABLE IV. Estimate of the number of electrons (δ) between the d-band edge and E_F for some stoichiometric fcc transition-metal hydrides based on the model discussed in Sec. IV. The symbols α, γ, and δ are defined in the text. The numerical estimate of δ is based on an approximate value of $\alpha-\gamma\simeq 1.5$.

	Co,Rh,Ir	Ni,Pd,Pt	Cu,Ag,Au
n	9	10	11
δ	$(\alpha-2)-\gamma$	$(\alpha-1)-\gamma$	$(\alpha-\gamma)$
Numerical estimate of δ	-0.5	0.5	1.5

features also have direct physical implications. For example, the hydride formation of noble metals would be unfavorable as the band energy contribution to the total energy of the hydride would be high due to the high Fermi energy.[28] Hydrides of elements in the same column as Pd in the Periodic Table have a small (Pauli-type) magnetic susceptibility and specific heat as the DOS at E_F would be low when the d-band edge is just passed, and hydrides Co, Rh, and Ir should have a relatively high magnetic susceptibility and specific heat. Thus we can see that qualitative predictions can be made easily with the simple equation (15).

Information about substoichiometric PdH_x can also be deduced from Eq. (15). For PdH_x ($n=10$, $\gamma=0.36$) we can write Eq. (15) as

$$\delta(x)=(\alpha-1)x-0.36\ . \tag{17}$$

As $\delta(x)$ decreased with x, this immediately suggests that the Fermi energy moves closer toward the d-band edge as the hydrogen concentration decreases. This is consistent with calculations on substoichiometric hydride.[17,19] Also, since $\alpha\sim 2$, $\delta(x)$ is negative at $x=0.25$. This means that there are unfilled d states in Pd_4H, which agrees with our explicit calculation of the system.

More quantitative comparison with experimental results can be made if we make an assumption (the strong bonding assumption) that the PdH_x DOS in the region between E_F and the d-band edge is very similar to that of PdH as long as x is close to 1. To determine the E_F of PdH_x, we count $\delta(x)$ electrons from the d-band edge, which is equivalent to counting a total of $11-\delta(1.0)+\delta(x)$ or $11-(\alpha-1)(1-x)$ electrons in the DOS of PdH. Note that in particular if we take $\alpha=2$, then $11-(\alpha-1)(1-x)=10+x$, and this reduces to the procedure taken by Papaconstantopoulos *et al.*, who have applied a rigid-band-like scheme to study the superconducting properties of PdH_x as a function x.[18] (Eastman *et al.*[7] also determined the E_F of $PdH_{0.6}$ by counting 10.6 electron states from the DOS of PdH.) This procedure was followed to test the validity of the assumption. Thus we plot in Fig. 10 $D(E_F)$ vs x where $D(E_F)$ of PdH_x is inferred from the DOS of PdH by counting $10+x$ electrons. On the same graph we also plot the $D(E_F)$ determined from Eq. (13) (with $\lambda=0$) with specific-heat data from experiments.[29–31] The agreement is good. The theoretically determined $D(E_F)$ for PdH_x of Papaconstantopolous *et al.*[18] and Zbasnik and Mahnig[17] show similar agreement. This justifies our assumption that due to strong bonding the part of DOS above the d-band maximum to the E_F does not change much with respect to x when x is close to 1. In this specific consideration, the rigid-band model is operationally equivalent to the strong bonding model with $\alpha=2$. However, there is no specific assumption of the form of the DOS of PdH_x below the d-band edge in the strong bonding model.

V. CONCLUSION

Using a fully self-consistent pseudopotential method, we have studied the electronic structure and

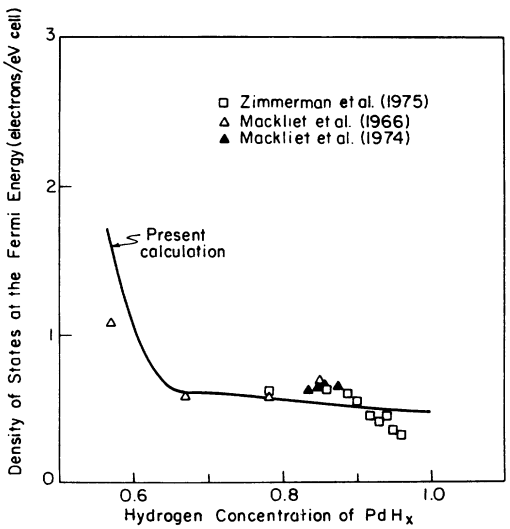

FIG. 10. Comparison of the density of states at Fermi energy of β-phase PdH_x as determined by the model discussed in Sec. IV with those determined by specific-heat experiments (with electron-phonon enhancement factor set to zero).

bonding character of PdH and Pd_4H. The study of PdH offers us direct information about the β-phase hydride, while the study of Pd_4H gives us insight into the behavior of the hydride system under a change of hydrogen content. From the study of band structure, DOS, and charge densities of these systems, we know that the main effect of H on the Pd host is to create a bonding band below the Pd d bands, regardless of concentration. The bonding state is well defined and essentially separated from the d bands. The proton is always screened by approximately one electron. The position of the bonding band and its angular momentum composition is very similar for PdH and Pd_4H. This indicates that hydrogen concentration and coordination number do not have a strong effect on the bulk hydride system as far as the nature of the Pd—H bond is concerned. The study of Pd_4H bonding charge densities shows that the Pd-H effective interaction is short ranged and does not quite extend beyond nearest neighbors.

The structure of the DOS near the d-band edge is similar for Pd, PdH, and Pd_4H. However, the Fermi energy and hence the DOS at E_F depends critically on the concentration of hydrogen impurities. This explains why physical properties such as magnetic susceptibility and specific heat depend strongly on the hydrogen content of the hydride system. Another important parameter which determines the position of the E_F is of course the number of electrons in the host metal. These key factors are all summarized in a simple physical picture introduced in Sec. IV. Operationally speaking, this is an electron counting procedure in which the role of the hydrogen is treated properly as a impurity that strips the host metal of electron states in the d bands to form a low-energy bonding state. It gives essentially the same predictions as the rigid-band model although the physics behind it is not the same. Qualitative predictions about Fermi-surface properties for substoichiometric PdH and hydrides of transition metals that are on adjacent columns in the Periodic Table can be obtained readily with this simple picture.

Note added in proof. After the submission of this paper, there are new experimental studies on the electronic structure of palladium hydride. Schlapbach and Burger[32] studied $PdH_{0.6}$ with UPS and x-ray photoelectron spectroscopy (XPS) while Bennett and Fuggle[33] studied $PdH_{0.8}$ with XPS. Both groups found that upon formation of the hydride the d bands become slightly narrower and are shifted away from the Fermi energy. Hydrogen induced states with considerable d character were observed below the d bands. Our calculations are thus in agreement with these new experiments. However, unlike previous experiments,[7] the observed hydrogen-induced states have weaker photoemission intensities and are at about 8 eV below the Fermi energy. Early data[7] placed these states at -5.4 eV whereas our calculations indicate that they are at about -6.5 eV. As remarked in Sec. III A, reducing the lattice constant leads to an expansion in the relative energy positions. $PdH_{0.6}$ and $PdH_{0.8}$ have lattice expansions of about 3%. By reducing the lattice expansion of PdH from 6% to 2% in our calculation, the Pd—H bonding band indeed moves down 1 eV to about 7.5 eV below E_F and is thus closer to the results from the latest experimental studies.

ACKNOWLEDGMENTS

We would like to thank Dr. C. Minot, who has made necessary modifications in the mixed-basis computer code at the initial stage, and Professor L. M. Falicov for useful comments on the model discussed in Sec. IV. Support for one of us (S.G.L.) by a Sloan Foundation fellowship is gratefully acknowledged. This work was supported by National Science Foundation Grant No. DMR-78-22465 and by a discretionary fund from the Director of the Lawrence Berkeley Laboratory.

[1]W. M. Muller, J. P. Blackledge, and G. G. Libowitz, *Metal Hydrides* (Academic, New York, 1968).

[2]*Hydrogen in Metals I,* Vol. 28 of *Topics in Applied Physics,* edited by G. Alefeld and J. Völkl (Springer, Berlin, 1978), *Hydrogen in Metals II,* Vol. 29 of *Topics in Applied Physics,* edited by G. Alefeld and J. Völkl (Springer, Berlin, 1978).

[3]F. A. Lewis, *The Palladium Hydrogen System* (Academic, New York, 1967).

[4]D. G. Westlake, C. B. Satterthwaite, and J. H. Weaver, Phys. Today 31, (11), 32 (1978).

[5]A. C. Switendick, Solid State Commun. 8, 1463 (1970); Int. J. Quantum Chem. 5, 459 (1971).

[6]W. Eberhardt, F. Greuter, and E. W. Plummer, Phys. Rev. Lett. 46, 1085 (1981).

[7]D. E. Eastman, J. K. Cashion, and A. C. Switendick, Phys. Rev. Lett. 27, 35 (1971).

[8]S. G. Louie, Phys. Rev. Lett. 42, 476 (1979).

[9]A. C. Switendick, Ber. Bunsenges. Phys. Chem. 76, 535 (1972).
[10]See, for example, *Hydrogen in Metals I*, Ref. 2, Chap. 3.
[11]S. G. Louie, K. M. Ho, and M. L. Cohen, Phys. Rev. B 19, 1774 (1979).
[12]K. M. Ho, M. L. Cohen, and M. Schlüter, Phys. Rev. B 15, 3888 (1977).
[13]L. Hedin and B. I. Lundqvist, J. Phys. C 4, 2064 (1971).
[14]See, for example, S. G. Louie and M. L. Cohen, Phys. Rev. B 13, 2461 (1976); W. E. Pickett, K. M. Ho, and M. L. Cohen, *ibid.* 19, 1734 (1979).
[15]D. J. Chadi and M. L. Cohen, Phys. Rev. B 8, 5747 (1973).
[16]G. Lehmann and M. Taut, Phys. Status Solidi B 54, 469 (1972).
[17]J. Zbasnik and H. Mahnig, Z. Phys. B 23, 15 (1976).
[18]D. A. Papaconstantopoulos, B. M. Klein, E. N. Economou, and L. L. Boyer, Phys. Rev. B 17, 141 (1978).
[19]D. A. Papaconstantopoulos, B. M. Klein, J. S. Faulkner, L. L. Boyer, Phys. Rev. B 18, 2784 (1978).
[20]M. Gupta and A. J. Freeman, Phys. Rev. B 17, 3029 (1978).
[21]C. D. Gelatt, Jr., H. Ehrenreich, and J. A. Weiss, Phys. Rev. B 17, 1940 (1978).
[22]F. Antonangeli, A. Balzarotti, A. Bianconi, E. Burattini, P. Perfetti, and N. Nistico, Phys. Lett. 55A, 309 (1975).
[23]See, for example, J. M. Ziman, *Principles of the Theory of Solids* (Cambridge University, Cambridge, 1964), Chaps. 4 and 10.
[24]J. J. Vuillemin and M. G. Priestly, Phys. Rev. Lett. 14, 307 (1965).
[25]W. A. Harrison, *Electronic Structure and the Properties of Solids* (Freeman, San Francisco, 1980) Chap. 20; J. Friedel, in *The Physics of Metals*, edited by J. M. Ziman (Cambridge University, New York, 1969).
[26]See, for example, Fig. 2 in M. Methfessel and J. Kübler, J. Phys. F 12, 141 (1982).
[27]A. R. Williams, J. Kübler, and C. D. Gelatt, Jr., Phys. Rev. B 19, 6094 (1979).
[28]This agrees with the augmented-spherical-wave calculation of Williams *et al.* (Ref. 27) where the results showed that the addition of hydrogen elevates the effective chemical potentials in the noble metals and thus causes the heats of formation of the noble metals to be positive.
[29]M. Zimmerman, G. Wolf, and K. Bohmhammel, Phys. Status Solidi A 31, 511 (1975).
[30]C. A. Mackliet and A. I. Schindler, Phys. Rev. 146, 463 (1966).
[31]C. A. Mackliet, D. J. Gillespie, and A. I. Schindler, Solid State Commun. 15, 207 (1974).
[32]L. Schlopbach and J. P. Burger, J. Phys. Lett. 43, L273 (1982).
[33]P. A. Bennett and J. C. Fuggle, Phys. Rev. B 26, 6030 (1982).